B. Wang
Department of Mechanical Engineering
Shanghai Jiao Tong University,
People's Republic of China

A. Zhang

J. L. Sun

School of Life Sciences and Technology,
Shanghai Jiao Tong University,
People's Republic of China

H. Liu
Department of Mechanical Engineering
Shanghai Jiao Tong University,
People's Republic of China

J. Hu
School of Life Sciences and Technology and
Shanghai Jiao Tong University,
People's Republic of China

L. X. Xu
School of Life Sciences and Technology,
Shanghai Jiao Tong University,
People's Republic of China and
School of Mechanical Engineering and Dept. of
Biomedical Engineering
Purdue University, West Lafayette, IN, USA

Study of SARS Transmission Via Liquid Droplets in Air

Microscale liquid droplets could act as the SARS carriers in air when released from an infected person through breathing, coughing, or sneezing. In this study, a dynamic model has been built to quantitatively investigate the effect of the relative humidity on the transport of liquid droplets in air using coupled mass transfer and momentum equations. Under higher relative humidity, the exhaled liquid droplets evaporate slowly. Larger droplets fall faster, which could reduce the probability of the droplets inhalation. This may be one of the most important factors that influence the SARS transmission in air.
[DOI: 10.1115/1.1835350]

Keywords: SARS, Relative Humidity (RH), Liquid Droplets, Air Transmission

Introduction

Since the Winter of 2002, severe acute respiratory syndrome (SARS) had affected nearly forty countries in all the continents, resulting in 812 deaths by July 1, 2003 as reported by the World Health Organization (WHO). The WHO suggested guidelines of prevention were executed in all the areas affected by SARS. But the outcome results were quite different. Vietnam became the first country that had successfully controlled the spread of SARS on April 28, 2003, and promising results were also emerged in Guangdong and Hong Kong of China, that suffered big outbreaks of SARS in February and March, 2003, respectively. On the other hand, at the same time, the situation was severe in Beijing and Shanxi while there were only a few cases reported elsewhere in China, such as Shanghai, Nanjing, Chongqing, and Hunan, etc.

The SARS infected travelers from the Guangdong province, where the initial outbreak took place, were the sources of new cases in other areas in China. Before the official announcement of the SARS outbreak in Beijing on April 26, 2003, there was not any control measure of travelers in most of the cities in China. The probability of the infected persons traveling to large cities like Beijing, Shanghai, and Nanjing, etc. was expected to be similar. Nevertheless, there existed significant difference in the number of the people infected in these cities. Besides other factors, the environmental factor could play an important role.

It is well known that three key factors are involved in the spread of infectious diseases: the source, the susceptible population, and the environment, based on epidemiology. According to the latest reports from WHO, some respiratory illnesses occur much less frequently when the temperature and the relative humidity are high. There are three facets in virus spreading in air that could be impacted by the relative humidity: transmission, viability, and susceptibility.

By analyzing the climate records of all the above mentioned areas, it was found that the relative humidity appeared to affect the transmission of the SARS virus. Higher relative humidity could have helped prevent the spread of the virus since in most of the large cities higher relative humidity (e.g., 70%–80%) during the period the infected population was found lower in mainland China. On the other hand, in Hong Kong and Singapore, despite the high relative humidity, the incidence of SARS was also high. This might be due to the fact that inside the air conditioned buildings the environment was well controlled and independent of the outdoor climate.

The major means through which the SARS spread was proven to be via person-to-person close contact. Transport of the virus via liquid droplets released from an infected person through breathing, coughing, or sneezing could be the source, especially in a closed and not-well-ventilated environment. The droplets released from the human body range from 0.5 to 200 μm in diameter [1]. The spread can happen as the outcoming droplets drift over a short distance (generally up to 3 feet) in air and inhaled by healthy persons. Small droplets up to 100 μm are highly probable of depositing throughout the respiratory tract, especially at pharynx and larynx [2], resulting in the next generation of infectors. If not inhaled, as the droplet evaporates in air and reduces to about 1–4 μm in diameter, the carried virus starts to break from it [3].

Like SARS, several other human infectious diseases spread in similar ways, such as Chickenpox, Influenza, Meningitis, Measles, Diphtheria, Pneumonia, Mumps, Tuberculosis, and Smallpox, etc.

Contributed by the Bioengineering Division for publication in the JOURNAL OF BIOMECHANICAL ENGINEERING. Manuscript received by the Bioengineering Division October 29, 2004; revised manuscript received September 8, 2004. Associate Editor: James Moore.

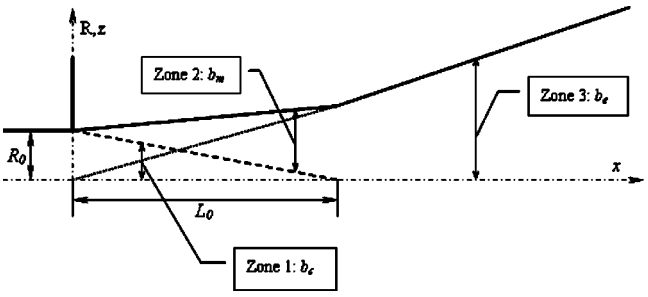

Fig. 1 Schematic of the jet flow field

All these diseases threaten the human life. It is worthwhile to study how the major environmental factors, e.g., the relative humidity, influence, the transport and the lifetime of airborne liquid droplets as virus carriers. This will help further our understanding of the disease transmission from the thermophysical point of view and provide effective environmental measures in the air conditioned hospitals, offices, etc. in the future. The main objective of the present work is to demonstrate how significantly the relative humidity can affect the transmission of SARS in air.

Physical Modeling

Of normal breath, cough, and sneeze, the outflow from the mouth or the nose may be treated as a jet flow with velocity ranging from several meters to tens of meters per second [1,4]. The diameter of the mouth is about several centimeters, and the corresponding Reynolds number is more than 30, at which Andrade [5] confirmed that the jet became turbulent. This critical Reynolds number depends on the shape of the exit jet profile, disturbance amplitude, and dimensionality. The instability mechanism involving nonlinear interaction of vortex sheets in the jet causes the transition of laminar to turbulent flow. The turbulent jet model is used in this study.

The modeled system consists of the liquid droplets released from a patient, water vapor, and the air. To simulate the droplet transport in air, the following assumptions are made:

1. the vapor–air flow from either the mouth or the nose is approximated as a 2D axisymmetric jet flow;
2. the flow is horizontal and its velocity distribution is uniform at the exit;
3. liquid droplets are uniformly distributed and transported by the flow. There are no interactions among the droplets;
4. the flow field is independent of the evaporation of liquid droplets;
5. the influences of the wall, ceiling, and any obstruction on the flow are neglected;
6. the exit flow is assumed to immediately equilibrate with the surrounding air, and a uniform temperature of 293 K is used for the surrounding air flow;
7. the relative humidity is about 70%–80% in the lung at the body temperature. It increases to unity as the jet flow temperature suddenly drops to the room temperature at the mouth exit.

Two-Dimensional Axisymmetric Turbulent Jet Model. Figure 1 shows the jet flow into still air used to mimic breathing, coughing, or sneezing of the human being. It is an axisymmetric jet and surrounded by the outer air flow. The radial axis is R and the axial coordinate is x. When investigating the droplet dynamics, only the vertical plane is considered, e.g., the x-z plane where z is the vertical coordinate. Since the flow is essentially at constant pressure and no obstruction assumed, it has constant momentum flux in any cross section:

$$M=\int_0^\infty \rho U^2 2\pi r dr=\rho U_0^2 \pi R_0^2, \tag{1}$$

where U_0 is the jet velocity at the mouth exit and R_0 is the approximated mouth radius.

A general turbulent jet model has three regions: (1) Zone 1, $x<L_0$, $R<b_c$, a conical region where the flow velocity is equal to the outlet velocity, $|\mathbf{U}|=U_0$, L_0 is the length of the region. The radius b_c linearly changes with x from R_0 to zero; (2) Zone 2, $x<L_0$, $b_c<R<b_c+b_m$, boundary layer region (or mixing region); (3) Zone 3, $x>L_0$, the developed region where the transverse velocity profiles are similar at different x and the velocity decay is assumed to be proportional to x^{-1} [6].

In the fully developed flow region, the axial mean velocity profiles are similar in each cross section. It has been demonstrated that the Gauss function profile fits well to the experimental data obtained in the studies of nozzle jet flows as [7,8]:

$$U=U_m \exp\left[-\left(\frac{R}{b_e}\right)^2\right]. \tag{2}$$

The centerline velocity U_m in Zone 3 is calculated based on the momentum conservation along the jet as:

$$\frac{U_m}{U_0}=\frac{1}{\sqrt{2}\varepsilon}\left(\frac{2R_0}{x}\right)=\frac{\sqrt{2}R_0}{\varepsilon x}. \tag{3}$$

From the experimental results by Albertson et al. [7], ε is a nondimensional number and takes the value of 0.114.

For the 2D problem, the velocity component in the x-z plane is:

$$|\mathbf{U}(x,z)|=U_m \exp\left[-\left(\frac{z}{\varepsilon x}\right)^2\right]=U_0\frac{\sqrt{2}R_0}{\varepsilon x}\exp\left[-\left(\frac{z}{\varepsilon x}\right)^2\right]. \tag{4}$$

At the end point of the jet core (Zone 1), one has the following relation $U_m=U_0$, e.g., $\sqrt{2}R_0/\varepsilon x=1$. The corresponding position is $L_0=\sqrt{2}R_0/\varepsilon$ and the radius is $b_c(x)=(1-x/L_0)R_0=R_0-\varepsilon x/\sqrt{2}$. In Zone 2, the velocity distribution is also described by the Gaussian function:

$$|\mathbf{U}|=U_0 \exp\left[-\left(\frac{R-b_c}{b_m}\right)^2\right], \quad b_c\leqslant R\leqslant b_c+b_m, \tag{5}$$

where b_c is the radius of Zone 1 and b_m of Zone 2 b_m is

$$b_m(x)=\sqrt{2}R_0\frac{x}{L_0}=\varepsilon x. \tag{6}$$

The boundary of Zone 2 is $b_e=b_c+b_m=R_0+\varepsilon x(1-\sqrt{2}/2)$.

Similarly, the vapor concentration (or the relative humidity) distribution in the jet region is obtained. It follows the Gauss distribution law but with a correction coefficient $f=1.12$, e.g., $c=c_m \exp[-R^2/(f\cdot b_e)^2]$ in the jet region (Zone 3) and $c=c_0 \exp[-(R-b_c)^2/(f\cdot b_m)^2]$ in the boundary layer (Zone 2) [9]. In a uniform temperature field, the relative humidity (RH) distribution obeys the same rule as the species concentration. The quantity c_0 is the vapor concentration at the mouth exit. The quantity c_m is the vapor concentration at the center line (x axis) of the jet. In the jet region, the value of c_m can be obtained using the flux conservation law as:

$$\int_0^\infty c|\mathbf{U}|2\pi r dr=c_0 U_0 \pi R_0^2. \tag{7}$$

The influence of the jet flow on the environmental RH value is negligible. For the area outside the jet flow region, the relative humidity is assumed to be c_∞, the environmental value.

Liquid Droplet Dynamics. The trajectory of a droplet is predicted by applying the force balance on the droplet, which is

written in a Lagrangian reference frame in the vertical plane. The droplet inertia is equated with the forces acting on the droplet, and could be written in the Cartesian coordinates as

$$\frac{d(m\mathbf{v}_x)}{dt} = -(\mathbf{v}_x - \mathbf{U})\mathbf{F}_{d,x}/|\mathbf{v}_x - \mathbf{U}|, \tag{8}$$

$$\frac{d(m\mathbf{v}_z)}{dt} = -mg - \mathbf{v}_z \cdot \mathbf{F}_{d,z}/|\mathbf{v}_z|, \tag{9}$$

where $\mathbf{v}_x$, $\mathbf{v}_z$ are the horizontal and vertical velocity components, respectively. g is the gravitational acceleration constant. The droplet is assumed to be spherical and its mass is $m=\rho_w(4/3\pi r^3)$. Due to evaporation, the droplet mass is a time variable. The magnitudes of the drag forces $\mathbf{F}_{d,x}$ and $\mathbf{F}_{d,z}$ are calculated from the following equations:

$$|\mathbf{F}_{d,x}| = \tfrac{1}{2}\rho_a|\mathbf{v}_x - \mathbf{U}|^2 C_{d,\text{sphere},x}\pi r^2, \tag{10}$$

$$|\mathbf{F}_{d,z}| = \tfrac{1}{2}\rho_a|\mathbf{v}_z|^2 C_{d,\text{sphere},z}\pi r^2. \tag{11}$$

The drag force coefficient $C_{d,\text{sphere}}$ is calculated according to [6]:

$$C_{d,\text{sphere},x} = \frac{24}{\text{Re}_x} + \frac{6}{1+\sqrt{\text{Re}_x}} + 0.4 \quad 0 \leqslant \text{Re}_x \leqslant 2\times 10^5, \tag{12}$$

$$C_{d,\text{sphere},z} = \frac{24}{\text{Re}_y} + \frac{6}{1+\sqrt{\text{Re}_z}} + 0.4 \quad 0 \leqslant \text{Re}_z \leqslant 2\times 10^5. \tag{13}$$

The relative Reynolds number for the flow around the droplet is defined as:

$$\text{Re}_x = \frac{\rho_a d_p|\mathbf{v}_x - \mathbf{U}|}{\mu_a}, \tag{14}$$

$$\text{Re}_z = \frac{\rho_a d_p|\mathbf{v}_z|}{\mu_a}, \tag{15}$$

where ρ_a is the air density, μ_a the air viscosity. The characteristic length takes the value of the diameter of the droplet, e.g., $d_p = 2r$.

When the particle size becomes comparable to the gas mean free path, the Cunningham correction should be applied to the Stokes drag force. Under the normal atmosphere pressure and temperature, the gas mean free path is 0.07 μm. Comparisons on the velocities of particles of different sizes under various force conditions can be found in [10]. It is shown that the Brownian forces become important for particles of 0.1–0.5 μm diameters. Thus for most droplets released from the human body, the Cunningham correction and Brownian forces can be neglected. The other forces contributing to the balance on the droplet such as the added mass force, the Basset history force and the pressure gradients are also neglected because of the large water/air droplet density ratio [11].

The position of the droplet (S_x, S_z) is calculated from:

$$\frac{dS_x}{dt} = |\mathbf{v}_x|, \tag{16}$$

$$\frac{dS_z}{dt} = |\mathbf{v}_z|. \tag{17}$$

Due to evaporation, the droplet radius decreases in the falling process, and the dynamics of the droplet is coupled with its mass reduction. Turbulent dispersion model is not implemented in the present jet flow model due to the lack of the velocity fluctuation details. Berlemont et al. [12] claimed that the influence of the turbulence or the velocity fluctuations on the mean droplet diameter and trajectories appeared to be very small, especially of the droplets with large radius, e.g., 100 μm, the initial diameter of the droplets modeled in this study. As the droplet evaporates, the influence may become significant.

Droplet Evaporation. The relation describing the evaporation rate of a stagnant pure water droplet is used [13]:

$$r\frac{dr}{dt} = F(T,p)\chi, \tag{18}$$

where $\chi = p_v/p_{v,sat} - 1$ is the ambient vapor fraction, $p_v(T)$ and $p_{v,\text{sat}}(T)$ the water vapor pressure in air and the vapor pressure under the saturation condition. For a rapid mixing model, the term $F(T,p)$ in Eq. (18) is given by:

$$F(T,p) = \left[\rho_w\left(\frac{R_w T}{D_v p_{v,\text{sat}}(T)} + \frac{L^2}{k_a R_w T^2}\right)\right]^{-1} \tag{19}$$

where D_v is the diffusivity of water vapor, k_a the thermal conductivity of air, L the latent heat, ρ_w the water density, and R_w the gas constant of water vapor. For the saturation water vapor pressure of a physiological liquid droplet, $p_{v,\text{sat}}(T)$ can be determined using the ideal solution assumption:

$$p_{v,\text{sat}}(T) = p_{v,\text{sat},w}(T)\times x, \tag{20}$$

where $p_{v,\text{sat},w}(T)$ is the saturation vapor pressure for pure water, x is the water mole fraction of the droplet:

$$x = \frac{V}{V + n_s v_w}, \tag{21}$$

where V is the volume of the droplet, n_s and v_w are the mole numbers of the salt ions and the water molar volume, respectively.

The droplet temperature is calculated with respect to time based on heat transfer through convection and evaporation:

$$mC_{p,d}\frac{dT}{dt} = hA(T_\infty - T) + \frac{dm}{dt}L, \tag{22}$$

where $C_{p,d}$ is the droplet specific heat, h the heat transfer coefficient, T_∞ the air temperature and A the surface area of the droplet. The heat transfer coefficient h is evaluated using the correlation by Ranz and Marshall [14]:

$$\text{Nu} = \frac{hd_p}{k_a} = 2 + 0.6\,\text{Re}_d^{1/2}\,\text{Pr}^{1/3}, \tag{23}$$

where, the Reynolds number is based on the particle diameter and the relative velocity as:

$$\text{Re}_d = \frac{\rho_a\sqrt{|\mathbf{v}_x - \mathbf{U}|^2 + |\mathbf{v}_z|^2}(2r)}{\mu_a}. \tag{24}$$

The Prandt1 number of the air is defined as $\text{Pr} = C_{p,a}\mu_a/k_a$.

When the relative Reynolds number is large, the flow effect needs to be taken into consideration. The correlation used for the correction of the relative velocity influence on the evaporation is [14]:

$$cfm = 1 + 0.3\,\text{Re}_d^{1/2}\,\text{Sc}^{1/3}, \tag{25}$$

where the Schmidt number $\text{Sc} = \mu_a/(\rho_a D_v)$. Considering the flow effect, the right-hand side of Eq. (18) is multiplied by the factor of cfm. The modified evaporation model can then be rewritten as:

$$F(T,p) = \left[\rho_w\left(\frac{R_w T}{D_v p_{v,\text{sat}}(T)} + \frac{L^2}{k_a R_w T^2}\right)\right]^{-1} cfm. \tag{26}$$

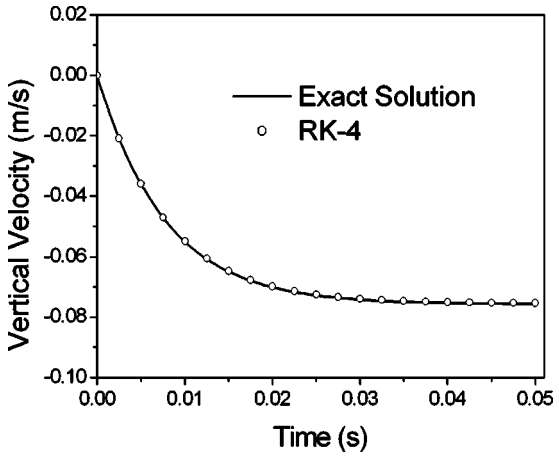

Fig. 2 Vertical velocity profile of the droplet in test case 1: $r_i = 25\ \mu$m, $V_i = 0$ m/s, without evaporation

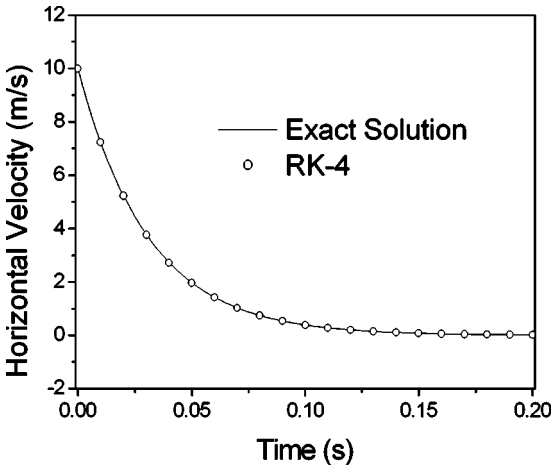

Fig. 3 Horizontal velocity profile of the droplet in test case 2: $r_i = 50\ \mu$m, RH=0.6, $V_i = 50$ m/s, with evaporation

For coughing and sneezing, it is necessary to apply this correction as shown in the next section. To solve the equations, the initial conditions are given as:

$$|\mathbf{v}_x|_{t=0} = V_i, \tag{27}$$

$$|\mathbf{v}_z|_{t=0} = 0, \tag{28}$$

$$T|_{t=0} = 310\ \text{K}, \tag{29}$$

$$r|_{t=0} = r_i, \tag{30}$$

$$S_x|_{t=0} = 0, \tag{31}$$

$$S_z|_{t=0} = \text{ManHeight}, \tag{32}$$

ManHeight takes the value of 1.7 m in all the calculations.

Results and Discussion

Model Validation. Equations (8), (9), (16)–(18), and (22) are solved using the fourth order Runge-Kutta method [15]. The mathematical model and the solution procedure are validated using the following two cases without any ambient flow: (1) free falling of a droplet without evaporation. The radius of the droplet is assumed to be small enough and the traditional Stokes drag force coefficient is $C_{d,\text{sphere}} = 24/\text{Re}_d$. The velocity is expressed as: $|\mathbf{v}_z(t)| = -2g\rho_v r_i^2/9\mu_a[1-\exp(-9\mu_a/2\rho_v r_i^2 t)]$. The result is shown in Fig. 2; (2) propagation of a droplet in the horizontal direction considering evaporation only. When the gravitational force is considered, an analytical solution can be obtained from the horizontal force balance as follows:

$$\frac{d\mathbf{v}_x}{dt} = -\frac{9}{2}\frac{\mathbf{v}_x\mu_a}{\rho_w r^2} = -\frac{9}{2}\frac{\mathbf{v}_x\mu_a}{\rho_w[r_i^2 + 2tF(T,p)\chi]}, \tag{33}$$

where the droplet radius is calculated from the evaporation model with the constant temperature assumption of the droplet ($T = 293$ K). The exact solution is found by solving the ordinary differential equations as:

$$|\mathbf{v}_x(t)| = V_i\left(\frac{r_i^2}{r_i^2 + 2F(T,p)t\chi}\right)^{9\mu_a/4F(T,P)\chi\rho_w}. \tag{34}$$

Shown in Figs. 2 and 3, the numerical simulations give almost identical results to those from the analytical solutions.

Justification of the Rapid Mixing Model. The rapid mixing model is used in this study, assuming the evaporation of droplets with uniform property and concentration. The concentration gradient may exist within the droplet due to rapid evaporation. It is necessary to justify whether the rapid mixing model is appropriate. The influence of the diffusion resistance on evaporation can be examined using the liquid Peclet number

$$\text{Pe} = \frac{dm/dt}{2\pi D_d D_v \rho_w}$$

[16], where dm/dt is the mass change due to evaporation, D_d is the droplet diameter, D_v is the diffusion coefficient and ρ_w the water density. As Pe$\rightarrow$0, the diffusion process is much faster than the evaporation. The concentration gradient in the droplet is negligible, which is the rapid mixing case.

After simplification, the expression of the Peclet number Pe $= r/D_v dr/dt$. The lifetime of the droplet is the key parameter. In this study, the evaporation lasts for about several seconds of small droplets (radius around 10–20 μm) and 10 s of droplets with 50 μm radius. The Pe number is on the order of 10^{-6}. Thus, the rapid mixing model can be used to describe the evaporation process.

Breathing. In this part of the study, ideal solution droplets are used to mimic the virus carriers from the human being via breathing. An ideal solution obeys the Raoult's law. The salt concentration in droplets is assumed to be 0.9% as the physiological value. Calculations of the trajectory are performed until the droplet radius is less than a half micron. In normal breath, the airflow through the nose and trachea is about several meters per second [1,4]. The flow is approximated by a jet flow of 3 cm radius. Since the maximum relative Reynolds number for normal breath is less than 0.3, and if the initial size and velocity of the droplet are $r_i = 15\ \mu$m and $V_i = 5$ m/s, respectively, then the steady state evaporation model can be used with good approximation. Trajectories of the droplets with initial radius of 10 μm and the jet flow velocities of 1, 2.5, and 5 m/s are shown in Fig. 4.

From the results, one can find that both the falling and horizontal flying distances increase with the relative humidity. The falling distance is less than 2 cm of the droplets with 10 μm radius, and 5 cm of those with 15 μm (results not shown). Droplets of this size can suspend in air after evaporation and follow the Brownian motion, which is temperature dependent. While carrying virus, these droplets can be dangerous since the probability of them being inhaled by people is high. As the initial jet flow velocity increases, droplets can travel several meters in the horizontal direction under the same relative humidity condition. The evaporation time is mostly within a couple of seconds mainly depending on the initial velocity and the relative humidity.

The relationship between the droplet size, and its falling distance and relative humidity is shown in Fig. 5. The gravity effect

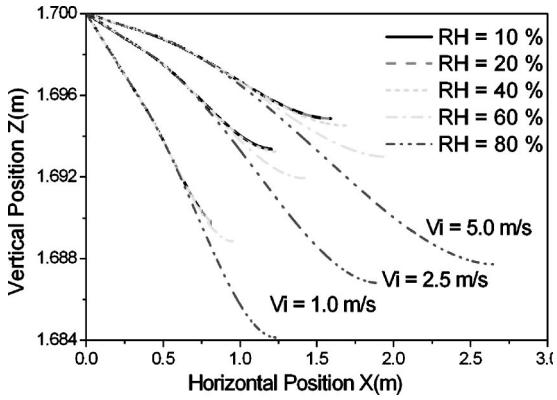

Fig. 4 Trajectories of the droplets with initial radius of 10 μm and the jet flow rates of 1.0, 2.5, and 5.0 m/s under different relative humidity conditions (RH)

is almost negligible when the RH is less than 60% since the droplets evaporate rapidly in air. The effect becomes much more significant as the RH increases to 80%. The longer falling distance in the vertical direction helps decrease the probability of the virus being inhaled by a person of similar height nearby. If such a person is walking by, and the air column inhaled is assumed to be 1 cm diameter, the possible reduction in the number of droplets inhaled by the person at the distance of 1.5 m is estimated under different relative humidity conditions, as shown in Table 1.

The results show that the relative humidity can significantly affect the inhalation of the droplets, e.g., the SARS carriers, in air. It suggests that higher relative humidity (around 80%) in Shanghai during April and May, could be one of the key factors for much less SARS transmission in the area. It should be noted that the solution of the droplets is assumed to be 0.9% NaCl as the physiological solution in the above simulation. Similar results have also been obtained using the intracellular fluid composition.

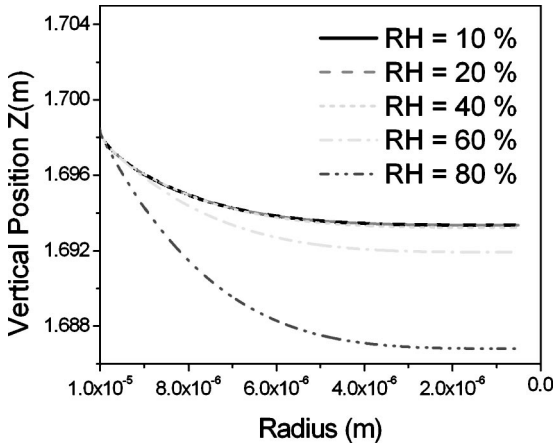

Fig. 5 Variation of the droplet radius versus the falling distance under different relative humidity conditions (RH) when the initial jet flow rate is 2.5 m/s

Table 1 Effect of the relative humidity (RH) and initial velocity on the number of droplets inhaled by a healthy person of the same height at the distance of 1.5 m from the infected individual

InitialVelocity (m/s)\RH	20%	40%	60%	80%
5.0	49%	45%	30%	0%
2.5	33%	32%	19%	0%
1.0	0%	0%	0%	0%

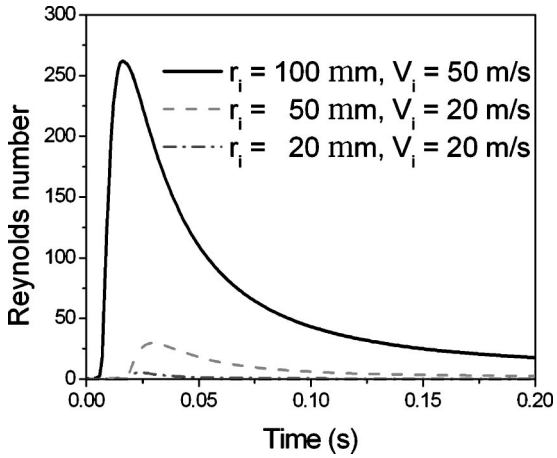

Fig. 6 Reynolds number of droplets with different initial sizes and velocity as they travel in air under the relative humidity condition RH=0.8

Coughing or Sneezing. When people cough or sneeze, the outgoing liquid droplets are much larger and at much higher initial velocities. In sneezing, millions of tiny droplets of water and mucus are expelled at up to 40 m per second [17]. The initial droplet radius is in the range of 10–100 μm, and it decreases rapidly in air because of evaporation. Due to the lack of the detailed statistical data, velocities of 10–50 m/s and radius of 20–100 μm are used in this study for simulation of liquid droplets from the human being via coughing or sneezing.

To examine the co-current jet flow assumption, the relative Reynolds numbers associated with different initial droplet sizes (r_i) and velocities (V_i) are calculated and given in Fig. 6. It is clear that the correction of the evaporation model [Eqs. (23) and (25)] is necessary in these cases since the Reynolds number and the value of cfm are both much larger than 1. Figure 7 shows the trajectories of droplets with initial radius of 20 μm. The trends are similar to those presented in Fig. 4 while the relative humidity has much greater effect on the final distance traveled in both directions. Of large droplets, the falling distance is almost the same which is independent of the initial jet velocity. The relationship of the droplet size, the falling distance, and the relative humidity is shown in Fig. 8. The influence of the relative humidity on the final falling distance is much greater than that of the initial velocity. As the initial droplet size increases, this influence becomes greater. Figure 9 shows the trajectories of a droplet with initial radius r_i =50 μm and velocity of 50 m/s under various relative humidity

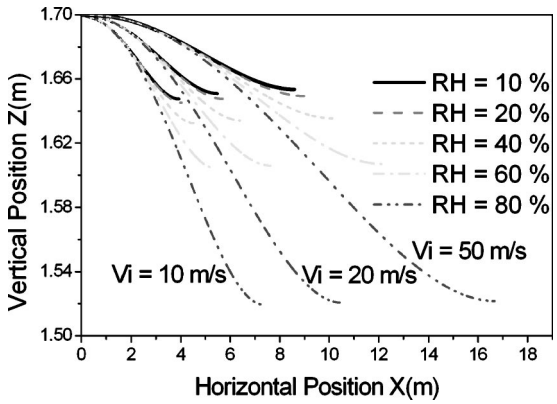

Fig. 7 Trajectories of the droplet with initial radius of 20 μm and the jet flow rates of 10, 20, and 50 m/s under different relative humidity conditions (RH)

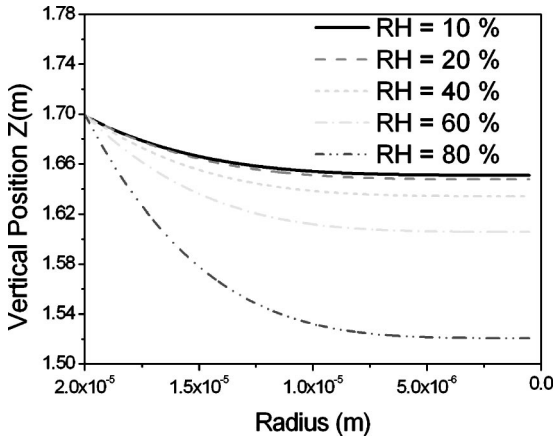

Fig. 8 Variation of the droplet radius versus the falling distance under different relative humidity conditions (RH) when the jet flow is 20 m/s

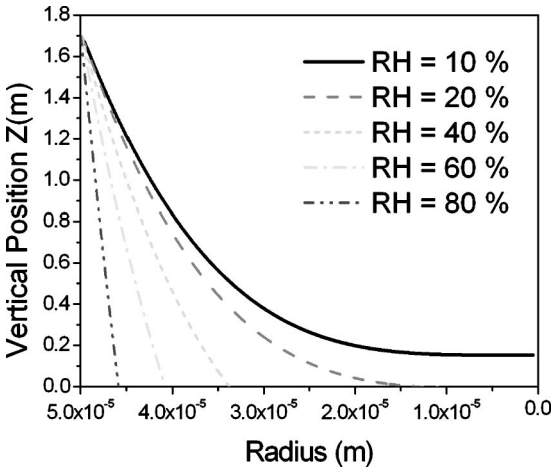

Fig. 10 Variation of the droplet radius versus the falling distance under different relative humidity conditions (RH) when the jet flow is 50 m/s

conditions. Under the conditions of RH=40% to RH=80%, the curves become vertical at the end because the droplets have fallen out of the jet flow region. The droplet lands on the ground before it becomes tiny enough to suspend in air, as shown in Fig. 10. The likelihood of these droplets to be inhaled by other people nearby is rare.

In comparison, the transmission of the droplet is recalculated without considering the influence of the temperature change due to evaporation (i.e., $T=T_\infty=293\,\mathrm{K}$). The falling distance is shorter. In the case of breathing, the final falling distance is 11% and 7% less under the conditions of the RH=0.1 and 0.8, respectively. In the case of coughing, the difference increases to about 20% and 10% less under RH=0.1 and 0.8, respectively, while it is 30% less under the RH=0.1 in the case of sneezing. These results indicate that it is necessary to take the temperature change into account in the transmission model, especially when the droplet size is large and the relative humidity is low. In the cases studied, the temperature reduces to about 285 K under the RH=0.1, while it almost keeps at the same value under the RH=0.8. The influence of the temperature change due to evaporation on the droplet transmission is more obvious in the environment with lower RH values, since significant heat transfer takes place during the rapid evaporation process.

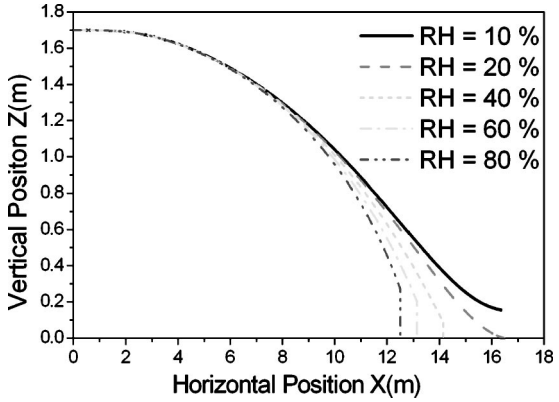

Fig. 9 Trajectories of the droplet with initial radius of 50 μm and the jet flow rate of 50 m/s under different relative humidity conditions (RH)

Conclusions

A two-dimensional model is built to predict the transmission of physiological liquid droplets in air. Normal breathing, coughing or sneezing have been simulated using turbulent jet flows at different initial velocities. With the evaporation model accounting for the dynamics of an isolated droplet in air, the influence of the relative humidity on the transmission distance and time is studied.

Small droplets (about 5–20 μm in radius) rapidly evaporate and the gravity effect is minimum. The contained viruses, if there are any, would then either suspend in air or attach to solid surfaces. Under the high relative humidity condition, the evaporation rate reduces which allows for a longer falling distance, especially of large droplets, which may help decrease the probability of the virus inhalation by other human beings in the vicinity. On the other hand, the longer transmission distance can also increase the possibility of virus attachment to the surrounding surfaces and thus decrease their suspension time in air. Large droplets (>50 μm in radius) land on the ground quickly under the high relative humidity (>40%) condition, while in dry air the droplets rapidly evaporate and suspend, which is more dangerous if containing viruses.

From the numerical results aforementioned, high relative humidity may help reduce the spread of viruses carried by liquid droplets in air. The steady jet flow assumption is used in the present work, and the horizontal transmission distance may be overestimated. In practice, deceleration of the jet flow can affect the transmission of droplets in air, especially in the horizontal direction. Nevertheless, the influence of the relative humidity is expected to be similar. In subsequent study, it is desirable to investigate the effect of the relative humidity on the viability of virus and the susceptibility of the human being, both playing important roles in the SARS transmission.

Acknowledgments

This work was supported by the special SARS funds from the Commission of Science and Technology of Shanghai Municipality and Shanghai Jiao Tong University.

Nomenclature

$C_{d,\mathrm{sphere}}$ = drag force coefficient
f = correction coefficient
$\mathbf{F}_{d,x}$, $\mathbf{F}_{d,z}$ = drag forces, N
n_s = mole number of the salt ions
$p_v(T)$ = water vapor pressure in air, Pa

$p_{v,\mathrm{sat}}(T)$ = vapor pressure of the droplet under saturation condition, Pa
$p_{v,\mathrm{sat},w}(T)$ = saturation vapor pressure for pure water, Pa
r_i = initial size of the droplet, m
R_0 = approximated mouth radius, m
Re = Reynolds number
RH = relative humidity
S_x, S_z = position of the droplet
Sc = Schmidt number
U = outlet velocity, m/s
U_0 = jet velocity at the exit, m/s
U_m = centerline velocity, m/s
V = volume of the droplet, m^3
V_i = initial velocity of the droplet, m/s
v_w = water molar volume, m^3
v_x = horizontal velocity components, m/s
v_z = vertical velocity components, m/s
x = water mole fraction in the droplet
χ = ambient fractional of super-saturation vapor

References

[1] Erdal, S., and Esmen, N. A., 1995, ''Human Head Model as an Aerosol Sampler: Calculation of Aspiration Efficiencies for Coarse Particles Using an Idealized Human Head Model Facing the Wind,'' J. Aerosol Sci., **26**, pp. 253–272.
[2] Stahlhofen, W., Rudolf, G., and James, A. C., 1989, ''Intercomparison of Experimental Regional Aerosol Deposition Data,'' J. Aerosol Med., **2**, pp. 285–308.
[3] http://helios.bto.ed.ac.uk/bto/microbes/airborne.htm
[4] Moskal, A., and Gradon, L., 2002, ''Temporary and Spatial Deposition of Aerosol Particles in the Upper Human Airways During Breathing Cycle,'' J. Aerosol Sci., **33**, pp. 1525–1539.
[5] Andrade, E. N., 1939, ''The Velocity Distribution in a Liquid-Into-Liquid Jet. Part 2: The Plane Jet,'' Proc. Phys. Soc. London, **51**, pp. 784–793.
[6] White, F. M., 1974, ''Viscous Fluid Flow,'' McGraw-Hill, New York, Chap. 3.
[7] Albertson, M. L., Dai, Y. B., Jensen, R. A., and Rouse, H., 1948, ''Diffusion of Submerged Jets,'' ASCE Proc. 74.
[8] Taylor, J. F., Grimmett, H. L., and Commings, E. W., 1951, ''Isothermal Free Jets of Air Mixing With Air,'' Chem. Eng. Prog., **4**, pp. 175–180.
[9] Yu, C. Z., 1987, ''Turbulent Injection,'' by higher education publishing company of China, Beijing, Chap. 2 (in Chinese).
[10] Ralph, A., 2001, ''Wet Electrostatic Precipitation Demonstrating Promise for Fine Particulate Control,'' The Magazine of Power Generation Technology, January.
[11] Crowe, C. T., Sharma, M. P., and Stock, D. E., 1977, ''The Particle-Source-in-Cell Model for Gas-Droplet Flows,'' ASME J. Fluids Eng., **99**, pp. 325–332.
[12] Berlemont, A., Grancher, M.-S., and Gouesbet, G., 1991, ''On the Lagrangian Simulation of Turbulence Influence on Droplet Evaporation,'' Int. J. Heat Mass Transfer, **34**, pp. 2805–2812.
[13] Xu, X., and Carey, V. P., 1991, ''Numerical Simulation of Mixing of Coaxial Air Flows With Condensation,'' Int. J. Heat Mass Transfer, **34**, pp. 1823–1838.
[14] Ranz, W. E., and Marshall, Jr., W. R., 1952, ''Evaporation From Drops, Part I,'' Chem. Eng. Prog., **48**, pp. 141–146.
[15] Steven, C. C., and Paymod, P. C., 2000, *Numerical Methods for Engineers*, 3rd ed., McGraw-Hill, New York.
[16] Burger, M., Schmehl, R., Prommersberger, P., Schaefer, O., Koch, R., and Witting, S., 2003, ''Droplet Evaporation Modeling by the Distillation Curve Model: Accounting for Kerosene Fuel and Elevated Pressures,'' Int. J. Heat Mass Transfer, **46**, pp. 4403–4412.
[17] http://www.diamondmedicalstaffing.com/pdfs/Standard Precautions 1.pdf